npg

ORIGINAL ARTICLE

Ascorbic acid enhances the cardiac differentiation of induced pluripotent stem cells through promoting the proliferation of cardiac progenitor cells

Nan Cao[1], Zumei Liu[1], Zhongyan Chen[1], Jia Wang[1], Taotao Chen[2], Xiaoyang Zhao[3], Yu Ma[1], Lianju Qin[1], Jiuhong Kang[2], Bin Wei[2], Liu Wang[3], Ying Jin[1, 4], Huang-Tian Yang[1, 4]

[1]Key Laboratory of Stem Cell Biology, Institute of Health Sciences, Shanghai Institutes for Biological Sciences (SIBS), Chinese Academy of Sciences (CAS) & Shanghai Jiao Tong University School of Medicine (SJTUSM), Shanghai 200025, China; [2]Laboratory of Molecular Cell Biology, Institute of Biochemistry and Cell Biology, SIBS, CAS, Shanghai 200031, China; [3]State Key Laboratory of Reproductive Biology, Institute of Zoology, CAS, Beijing 100101, China; [4]Shanghai Stem Cell Institute, SJTUSM, Shanghai 200025, China

Generation of induced pluripotent stem cells (iPSCs) has opened new avenues for the investigation of heart diseases, drug screening and potential autologous cardiac regeneration. However, their application is hampered by inefficient cardiac differentiation, high interline variability, and poor maturation of iPSC-derived cardiomyocytes (iPS-CMs). To identify efficient inducers for cardiac differentiation and maturation of iPSCs and elucidate the mechanisms, we systematically screened sixteen cardiomyocyte inducers on various murine (m) iPSCs and found that only ascorbic acid (AA) consistently and robustly enhanced the cardiac differentiation of eleven lines including eight without spontaneous cardiogenic potential. We then optimized the treatment conditions and demonstrated that differentiation day 2-6, a period for the specification of cardiac progenitor cells (CPCs), was a critical time for AA to take effect. This was further confirmed by the fact that AA increased the expression of cardiovascular but not mesodermal markers. Noteworthily, AA treatment led to approximately 7.3-fold (miPSCs) and 30.2-fold (human iPSCs) augment in the yield of iPS-CMs. Such effect was attributed to a specific increase in the proliferation of CPCs via the MEK-ERK1/2 pathway by promoting collagen synthesis. In addition, AA-induced cardiomyocytes showed better sarcomeric organization and enhanced responses of action potentials and calcium transients to β-adrenergic and muscarinic stimulations. These findings demonstrate that AA is a suitable cardiomyocyte inducer for iPSCs to improve cardiac differentiation and maturation simply, universally, and efficiently. These findings also highlight the importance of stimulating CPC proliferation by manipulating extracellular microenvironment in guiding cardiac differentiation of the pluripotent stem cells.

Keywords: induced pluripotent stem cells; ascorbic acid; cardiomyocytes; cardiac progenitor cells
Cell Research (2012) **22**:219-236. doi:10.1038/cr.2011.195; published online 6 December 2011

Introduction

Establishment of embryonic stem cell (ESC)-like cells (also know as induced pluripotent stem cells or iPSCs)

by the reprogramming of adult somatic cells with a few defined transcription factors provides a fascinating route to generate patient-specific pluripotent cells as disease models and drug-testing systems [1-3]. Improvement of cardiac function by the transplantation of iPSC-derived cardiomyocytes (iPS-CMs) after myocardial infarction in animal models [4] suggests a potential of using iPSCs in patient-specific cardiac regeneration [5, 6]. However, to realize these application potentials, establishment of a highly efficient and easily practicable differentiation system is one of the prerequisites.

Cardiogenesis is a well-organized process tightly regulated by key developmental signals and extracellular microenvironment [7, 8]. Although cardiomyocytes are successfully generated from mouse (m) [9, 10] and human (h) [11, 12] iPSCs *in vitro*, the cardiac differentiation efficiency remains very low [5]. Several attractive approaches focusing on the manipulation of critical signaling pathways to improve the cardiac differentiation efficiency of iPSCs have been reported currently [13-15], while little is known about the contribution of manipulating extracellular microenvironments to the process of cardiac differentiation from iPSCs.

Another important obstacle hampering the utilization of iPSCs is the high interline variability in cardiac differentiation efficiency [11, 12, 16], with some of the lines even showing no cardiac differentiation properties *in vitro* [17]. Therefore, a highly efficient and universal system must be developed to overcome or minimize such variations before the extensive use of iPSCs.

In addition, iPS-CMs have been proved to be less mature than those from ESCs or fetal hearts, reflected by the delayed development of sarcoplasmic reticulum and lower responses to β-adrenergic stimulus [18, 19]. Such immaturity not only results in ineffective contractile force generation but may also lead to arrhythmia [6]. Thus, it is important to develop approaches to facilitate the maturation of iPS-CMs.

ESC-derived cardiac progenitor cells (CPCs) are capable of populating multiple lineages of the heart and offer exciting alternative avenues for cardiac regeneration [20], while iPSCs are a novel source to generate individual-specific CPCs [21, 22]. Although CPCs have been identified by multiple markers [20], the mechanism underlying the renewal and differentiation of CPCs is poorly understood, and proper methods to efficiently obtain and expand iPSC-derived CPCs *in vitro* remain challenging.

Accumulating evidences have shown that iPSCs are similar but not fully identical to ESCs and are considered a unique subtype of pluripotent cells [2, 3, 23]. Previous studies on ESC differentiation have provided knowledge and methods for directing cardiac differentiation of ESCs [7, 24] and will facilitate the development of optimal approaches for the cardiac differentiation of iPSCs. However, it is unclear whether these knowledge and methods can be fully applied to iPSCs. Kattman *et al.* [14] developed an efficient cardiac differentiation approach recently by adjusting the levels of Activin/Nodal and BMP signaling. They found distinct responses of iPSCs to cytokine stimulation compared with ESCs. Thus, systematic and detailed analyses on iPSCs with the knowledge learned from ESC differentiation are required.

Ascorbic acid (AA) has been demonstrated to promote the cardiac differentiation of ESCs [25-27] and is applied in several reported protocols in both ESCs and iPSCs [14, 15, 28]. However, the exact roles of AA in the cardiac differentiation of iPSCs and the underlying mechanism have not yet been assessed.

To identify suitable inducers for iPSC-CMs, we here systematically screened sixteen cytokines and chemical compounds reported to facilitate the cardiac differentiation of ESCs. We found that only AA robustly and reproducibly enhanced cardiac differentiation of iPSCs even in the lines without spontaneous cardiogenic potential. Optimized treatment of AA led to approximately 7.3-fold (miPSCs) and 30.2-fold (hiPSCs) increases in the relative abundance of cardiomyocytes. Moreover, the structural and functional maturation of iPS-CMs were improved by AA treatment, providing the first successful pro-maturation method that works on iPS-CMs to our knowledge. Then we analyzed the mechanisms underlining AA-promoted cardiac differentiation and showed that AA specifically enhanced the proliferation of CPCs via the MEK-ERK1/2 pathway through manipulating collagen synthesis. Furthermore, isolated CPCs expanded more rapidly in the presence of AA. Therefore, we have developed a universal, economical, and efficient system for producing CPCs and functional iPS-CMs. Our findings also provide new insight into the mechanisms of AA-promoted cardiac differentiation and collagen-enhanced CPC proliferation.

Results

AA consistently and robustly enhances cardiac differentiation of iPSCs

To understand more about the ability of cardiomyocyte inducers of ESCs in the facilitation of cardiogenesis of iPSCs, we first systematically screened 16 cytokines and chemical components that were reported to promote the cardiac differentiation of ESCs following the optimized concentration and window in six miPSC lines generated from various origins or developed by different methods (Supplementary information, Table S1). Utilizing the classical hanging drop-based embryoid body (EB) model, we identified that only AA showed consistent and robust cardiac-inducing effects among different iPSC lines, even in the lines without spontaneous cardiac differentiation potential by evaluating the profile of Ebs containing beating clusters (Supplementary information, Figure S1), a typical phenomenon for the presence of functional cardiomyocytes [29].

Characteristics of AA-induced cardiac differentiation in miPSCs

To further determine the effects of AA and dissect its mechanisms in promoting cardiomyocytes differentiation, we utilized miPSC lines IP20D-3 generated by retroviral delivery of four transcription factors, Oct4, Sox2, Klf4, and c-Myc (iPS-4F) [30] and iPS-R-B1 (without c-Myc, iPS-3F) as two representative cell lines. Undifferentiated iPSCs showed typical ESC-like morphology, high alkaline phosphatase activity, and universally expressed pluripotent markers Oct4 and SSEA1 (Supplementary information, Figure S2A). Fluorescence-activated cell sorting (FACS) analysis further confirmed that > 86% cells expressed SSEA1 (Supplementary information, Figure S2B). RT-PCR analysis detected the expressions of key endogenous pluripotent genes *Oct4*, *Sox2*, *Nanog*, and *Rex1* in both iPSC lines but not the exogenous transgenic factors (Supplementary information, Figure S2C).

To characterize the effect of AA in the cardiogenesis of iPSCs, cells were treated with AA from 0.2 to 250 μg/ml for 10 days from the initiation of differentiation. The percentage of contracting EBs and the relative expression level of cardiac gene *Tnnt2* significantly increased in a concentration-dependent manner and reached a peak around 50 μg/ml (Figure 1A). To determine the exact stage in which AA takes effect, we then systematically added AA (50 μg/ml) during early-phase (day 0-2), mid-phase (day 2-6), or late-phase (day 6-10) of iPSC differentiation (Figure 1B) both individually and throughout. AA treatment during differentiation day 2-10 significantly increased cardiac differentiation equivalent to the treatment during the entire differentiation period (Figure 1B, 3 and 6). Consistently, AA treatment during day 0-2 failed to promote cardiac differentiation of both iPSC lines (Figure 1B, 1). Moreover, AA treatment during day 0-6 or 2-6 fulfilled 76%-85% or 72%-79% of its maximal cardiac induction potential, whereas this effect was totally disappeared by withdrawal of AA during day 2-6 (Figure 1B, 2, 4 and 5). These results reveal that the midphase (day 2-6), a critical phase for CPC specification [20], is the most crucial period for AA to inure.

Then profiles of contracting EBs with or without AA treatment were further examined. Spontaneously beating cardiomyocytes were visible at day 7 without AA treatment and 38% (iPS-4F) to 54% (iPS-3F) of the EBs developed contracting clusters 4-5 days later and remained stable up to 21 days examined, whereas contracting EBs were robustly enhanced to 90%-100% 1-3 days after plating in AA-treated cells (Figure 1C), implying the faster development of AA-induced cardiomyocytes. An approximate 7.3-fold increase of cardiomyocyte for-

mation in the total population of AA-treated EBs was further confirmed by intracellular staining of the cardiac isoform of Troponin T (cTnT) in FACS analysis at day 15 (Figure 1D). Consistently, larger beating areas were observed in AA-treated EBs and further consolidated by the immunostaining analysis of specific myofilamental protein markers α-actinin and cTnT (Figure 2A). AA treatment always led to a synchronous beating of the entire EB (Figure 2A and Supplementary information, Movie SI-SIV). In addition, AA-promoted cardiac differentiation was also observed in an auto-aggregated model, which allowed the scalable production of EBs, as well as in a serum-free differentiation system (Supplementary information, Figure S3).

Next, we examined whether AA treatment affects the sarcomeric organization of iPSC-CMs by immunostaining of α-actinin and cTnT on day-18 iPS-CMs. AA-induced cardiomyocytes showed better-organized cross-striated myofilaments compared with the control ones (Figure 2B), suggesting that the sarcomeric organization and structural maturation of iPS-CMs is enhanced by AA treatment.

AA promotes cardiovascular but not mesodermal differentiation of iPSCs

To elucidate the critical stage for AA in promoting cardiomyocyte differentiation of iPSCs, we then analyzed the expression of pluripotent, mesoderm, cardiac precursor, and cardiomyocyte genes by RT-PCR and quantitative RT-PCR (qPT-PCR). AA-treatment clearly increased the expression of cardiac transcription factors *Gata4*, *Isl1*, and *Mef2c* in both iPSC lines, whereas the expression of pluripotency markers *Oct4*, *Nanog*, and *Rex1* decreased more rapidly with the time of iPSC differentiation (Figure 3A). The expression levels of cardiac muscle-specific genes *Myl2*, *Myl7*, *Myh6*, and *Tnnt2* also remarkably upregulated in AA-applied cells (Figure 3A). Concomitantly, genes major encoding cardiac function regulators and calcium-handling proteins, including *Nppa*, *Slc8a1*, *Gja1*, *Cacna1a*, and *Ryr2*, were more intensively induced by AA treatment (Figure 3A). qRT-PCR analyses further revealed that the expression levels of mesodermal genes *Brachyury* and *Flk1* remained unchanged in AA-treated EBs compared with the corresponding controls ($P > 0.05$, Figure 3B, upper panels), whereas the expression of cardiac genes, *Nkx2-5* and *Tbx5*, was remarkably increased from differentiation day 5, a critical time point for CPC specification (Figure 3B, lower panels). In addition, AA also moderately increased the expressions of smooth-muscle markers *Myh11* and *Mkl2*, endothelial markers *Pecam1* and *Cdh5*, but not hematopoietic markers *Gata1* and *Cbfa2t3* (Figure 3A),
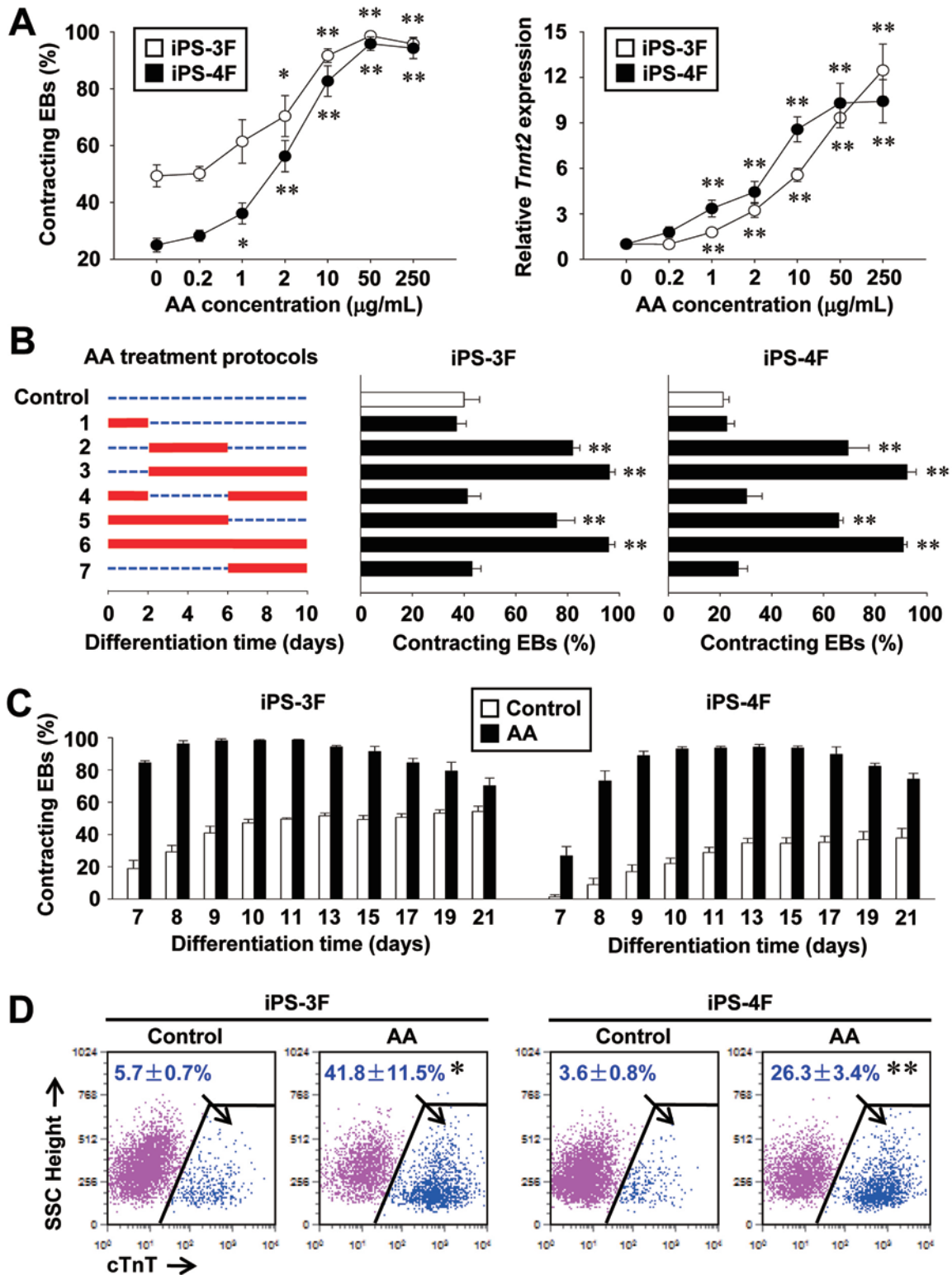
Figure 1 AA robustly enhances cardiogenesis of 3F and 4F miPSCs. **(A)** Concentration-dependent relationships of AA. Data were collected at day 10. **(B)** Time windows for AA-promoted cardiac differentiation. Left panel, schematic diagram of the differentiation protocols; middle and right panels, corresponding efficiency in 3F and 4F lines. **(C)** Differentiation profile of cardiomyocytes in both iPSC lines. **(D)** Percentages of cTnT$^+$ cardiomyocytes at day 15 in the total population derived from both iPSC lines with or without AA treatment. $n = 3$ each. Data are expressed as means ± SEM. *$P < 0.05$, **$P < 0.01$ vs control.
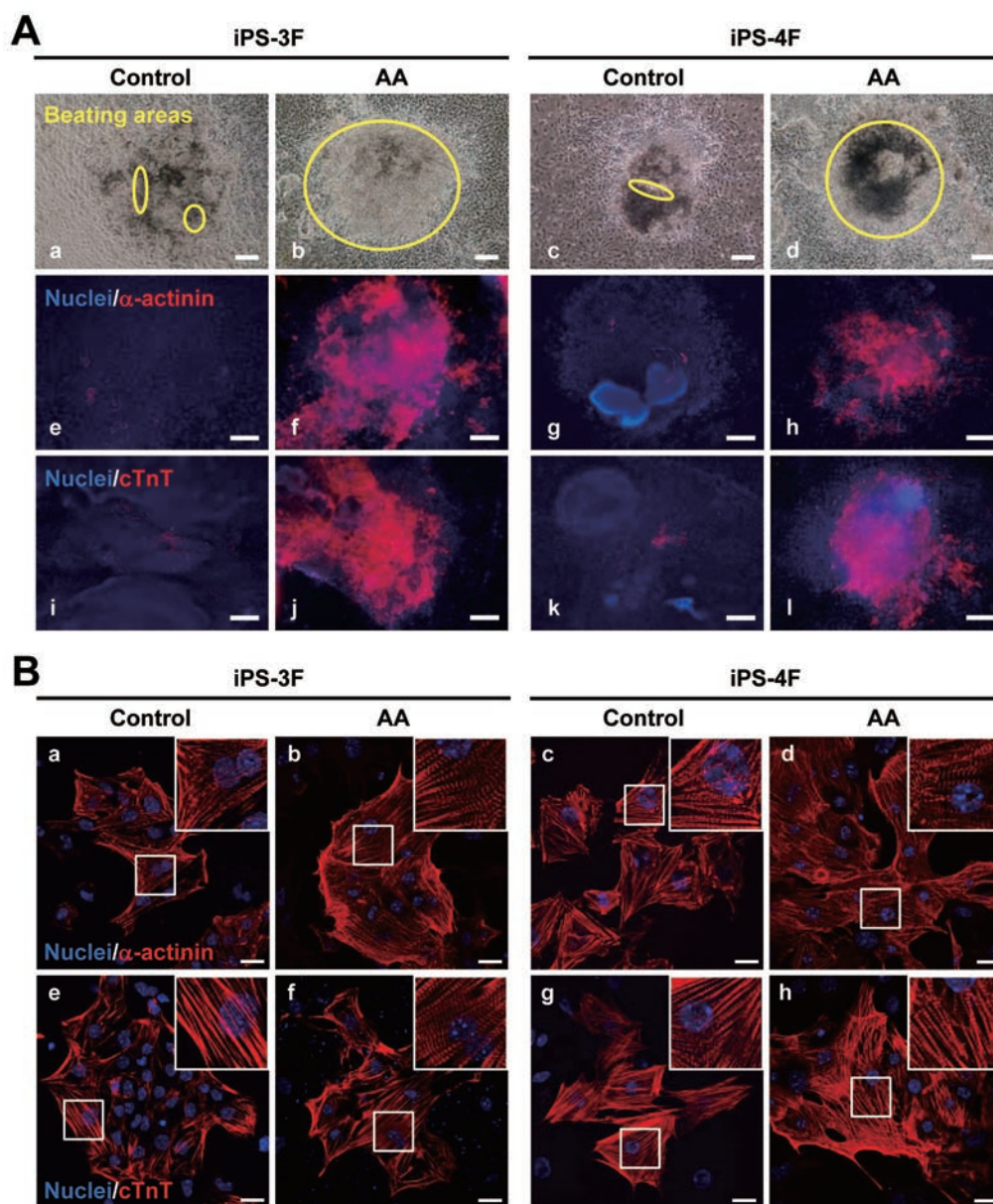
Figure 2 AA increases the content and improves the sarcomeric organization of iPS-CMs. **(A)** Representative images showing increased beating areas (a-d) and the content of α-actinin$^+$ (e-h) or cTnT$^+$ (i-l) cardiomyocytes in day-10 EBs treated with AA. Scale bars = 100 μm. **(B)** Sarcomeric structure analysis of the day-18 iPS-CMs by α-actinin and cTnT staining. The insets were magnifications of the framed areas showing more organized cross-striation alignment of sarcomeres in AA-induced iPS-CMs. Scale bars = 25 μm. Nuclei were counterstained with Hoechst33258 (blue).

which were further confirmed by FACS analysis of α-SMA (smooth muscle), CD31 (endothelial), and CD41 (hematopoietic, Supplementary information, Figure S4). However, the expression of endodermal (*Sox17* and *Afp*) and ectodermal markers (*Sox1* and *Nestin*) was not obviously affected by AA treatment (Figure 3A). Taken together with the observation of AA without effects during differentiation day 0-2 (Figure 1B), these data suggest that AA specifically increases cardiovascular but not mesoderm differentiation of iPSCs.

AA treatment rescues innate cardiogenic deficiency of iPSC lines

iPSC lines display a huge variation in their cardiac differentiation capacity [11, 12, 16, 17]. Such phenomenon was observed in six iPSC lines used for the preliminary
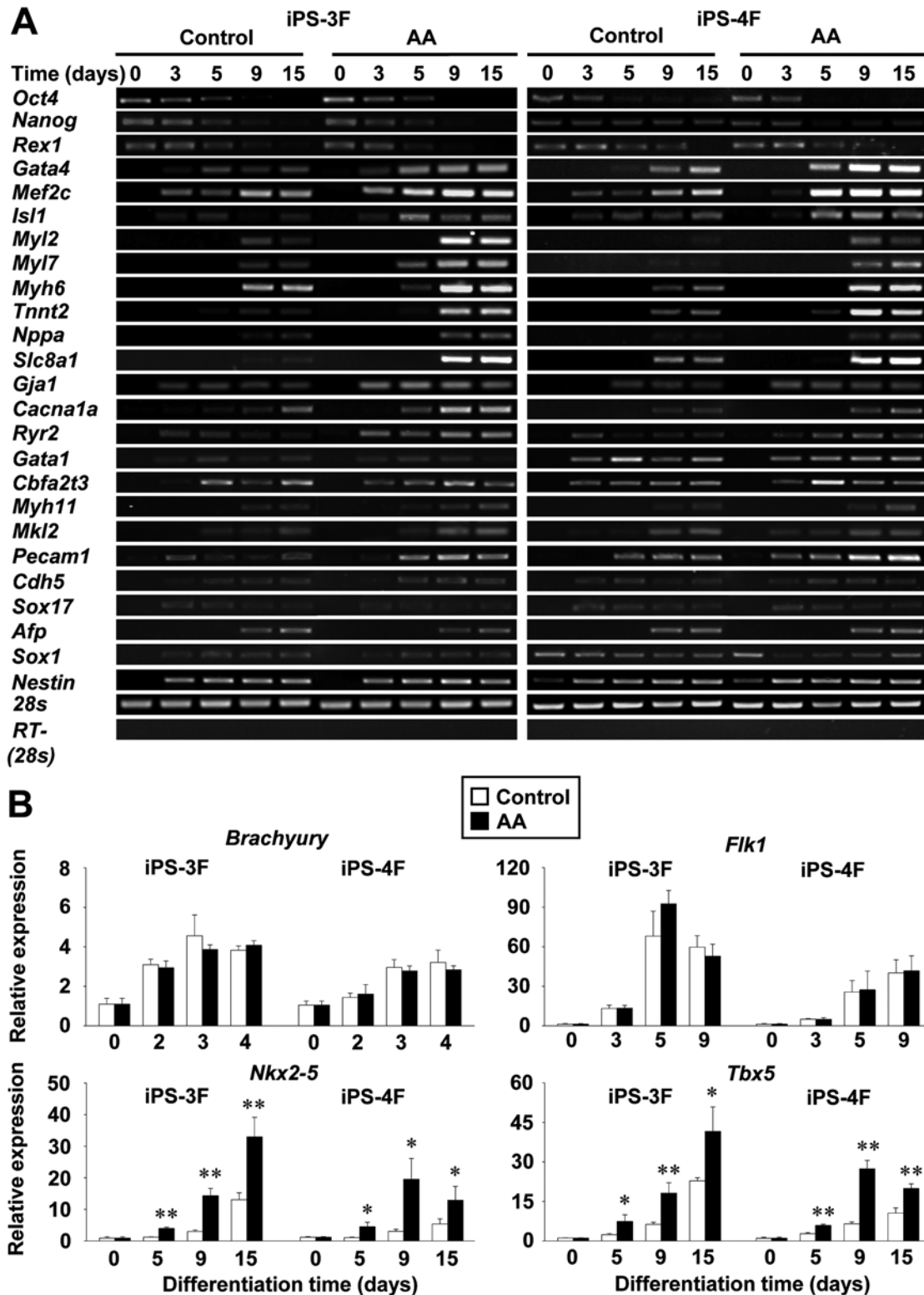
Figure 3 AA increases the expression of cardiac genes. **(A)** RT-PCR analysis showing the particular upregulation of cardiac genes in AA-stimulated EBs compared with the untreated ones. **(B)** Quantitative RT-PCR analysis indicated the increased expression of cardiac progenitor but not mesodermal transcripts (n = 3). Data are expressed as means ± SEM. *P < 0.05, **P < 0.01 vs control.

screening of cardiomyocyte inducers in our study and was minimized after AA treatment (Supplementary information, Figure S1), indicating that AA might overcome cell line variation in the cardiac differentiation. To confirm this, we then tested AA on five other lines generated from various origins and methods (Supplementary information, Table S1) by examining the profile of contracting EBs. AA treatment induced cardiac differentiation of all tested cell lines originally without spontaneous development of beating cardiomyocytes (Figure 4A). Further analyses were performed on three representative iPSC lines established by different laboratories [30-32]. The control EBs from all three lines showed no spontaneous contractility, whereas evident beating activities were reproducibly observed in AA-treated EBs with an increasing tendency from differentiation day 9-11 (Figure 4B). Coordinately, the expression of key cardiac genes *Nkx2-5* and *Tnnt2* was robustly increased in AA-treated EBs during differentiation (Figure 4C) and the occurrence of α-actinin$^+$ or cTnT$^+$ cardiomyocytes was only detected in AA-treated EBs at day 15 from all three iPSC lines (Figure 4D). These data indicate that AA induces cardiac differentiation in iPSC lines without intrinsic cardiac potential *in vitro* and might be useful in overcoming cell line variation in the cardiac differentiation efficiency.

AA treatment improves maturation of iPS-CMs reflected by enhanced responses to β-adrenergic and muscarinic stimulations

Because AA was observed to enhance the sarcomeric organization and structural maturation of iPS-CMs (Figure 2B), we then tested whether AA could improve the functional maturity of iPS-CMs by characterizing action potentials (APs) of iPS-CMs with or without AA treatment and detected their responses to β-adrenergic and muscarinic stimulations, critical signaling pathways in cardiomyocytes. iPS-CMs at differentiation day 16-18 displayed nodal-like, atrial-like, and ventricular-like APs in both control (data not shown) and AA-treated groups (Figure 5A). AA treatment did not affect the beating frequency (BF), amplitude (APA), maximum rise rate (V_{max}), and rate of diastolic depolarization (DD) of APs, as well as the AP duration at 50% repolarization (APD_{50}) in iPS-4F cells, whereas the DD was increased by AA treatment in iPS-3F cells (Supplementary information, Table S2). β-adrenergic agonist isoproterenol (Iso) at 10 nmol/l significantly increased the BF, DD, APA, and V_{max} of the APs in iPS-CMs, whereas carbachol (Cch), a synthetic muscarinic agonist, showed opposite negative effects at 1 μmol/l in both cell lines. Strikingly, these responses were both much stronger in AA-applied cells (Figure 5B). In addition, AA-treated cells showed higher basal

intracellular free Ca^{2+} concentration ([Ca^{2+}]$_i$), APA, upstroke V_{max}, and decay rate of Ca^{2+} transients (Supplementary information, Figure S5A), as well as stronger responses to 10 nmol/l Iso characterized by larger increases of the Ca^{2+} transient parameters in both cell lines (Figure 5C and 5D), implying a larger internal store and more rapid operation of Ca^{2+} in these cells. This was supported by the dramatic increased expression of *Ryr2*, *Atp2a2*, *Pln* and *Gja1* encoding crucial calcium-handling and gap junction proteins (Supplementary information, Figure S5B) and their corresponding proteins (Supplementary information, Figure S5C) in purified AA-treated day-18 iPS-CMs by tetramethylrhodamine methyl ester perchlorate (TMRM) staining [33]. These data demonstrate that AA treatment improves the maturation of iPS-CMs and enhances the ability of iPS-CMs to respond to critical functional regulations.

AA-promoted cardiac differentiation through increasing collagen synthesis

To explore the specific mechanism underlying AA-stimulated cardiac differentiation of iPSCs, we then investigated whether the cardiomyocyte-promoting effect of AA is attributed to its antioxidative property. Treatment with alternative antioxidants such as vitamin B1 (Vb1), reduced gluthatione (GMEE), and N-acetyl-L-cysteine (NAC), failed to mimic the effect of AA on the cardiac differentiation (Supplementary information, Figure S6A), suggesting that the cardiomyocyte-promoting role of AA is independent of its antioxidative property. Since collagen synthesis has been shown to be required for AA-enhanced cardiac differentiation of mESCs [25], we then analyzed the effect of AA on collagen synthesis and found significant increases in the expression of collagen genes *Col1a1* and *Col4a1* from differentiation day 5-15 in AA-treated iPSCs (Supplementary information, Figure S6B). Immunostaining results further confirmed the robust increased expression of type IV collagen (Col IV), which has been shown to facilitate the development of cardiovascular cells from iPSCs [10], in AA-applied EBs (Figure 6A). To further clarify the role of collagen synthesis in AA-induced cardiac differentiation of iPSCs, we stably downregulated the expression of Col I or Col IV in iPS-3F and iPS-4F lines by lentiviral delivery of small interfering RNAs (siRNAs, Supplementary information, Figure S7A). The AA-promoted cardiac differentiation was partially hampered by either downregulation of Col I or Col IV and the knockdown of both Col I and Col IV had an additive effect (Supplementary information, Figure S7B), suggesting that various types of collagens are required for AA-enhanced cardiac differentiation. We thus utilized
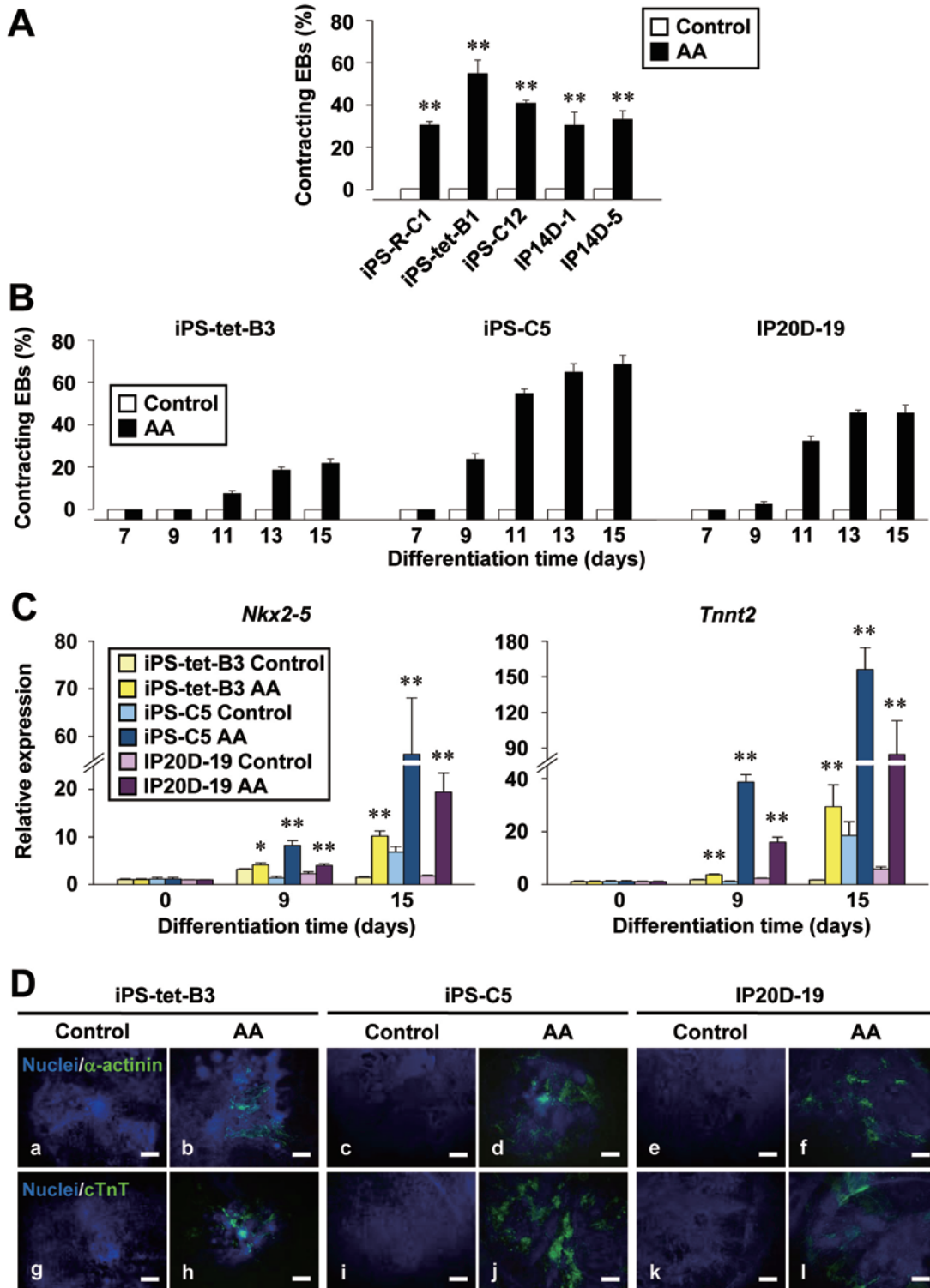
Figure 4 Rescue of innate cardiac deficiency by AA treatment. **(A)** AA induced the development of contracting EBs in other 5 iPSC lines without spontaneous cardiogenic potential. Data were collected at day 10. **(B)** Differentiation profile of cardiomyocytes in three representative iPSC lines. **(C)** Quantitative RT-PCR analysis of the expression level of cardiac genes. **(D)** Immunostaining showing the only emergence of α-actinin[+] and cTnT[+] cardiomyocytes in AA-treated EBs at day 10. Scale bars = 100 μm. Nuclei were counterstained with Hoechst33258 (blue). Data are expressed as means ± SEM. *$P < 0.05$, **$P < 0.01$ vs control.
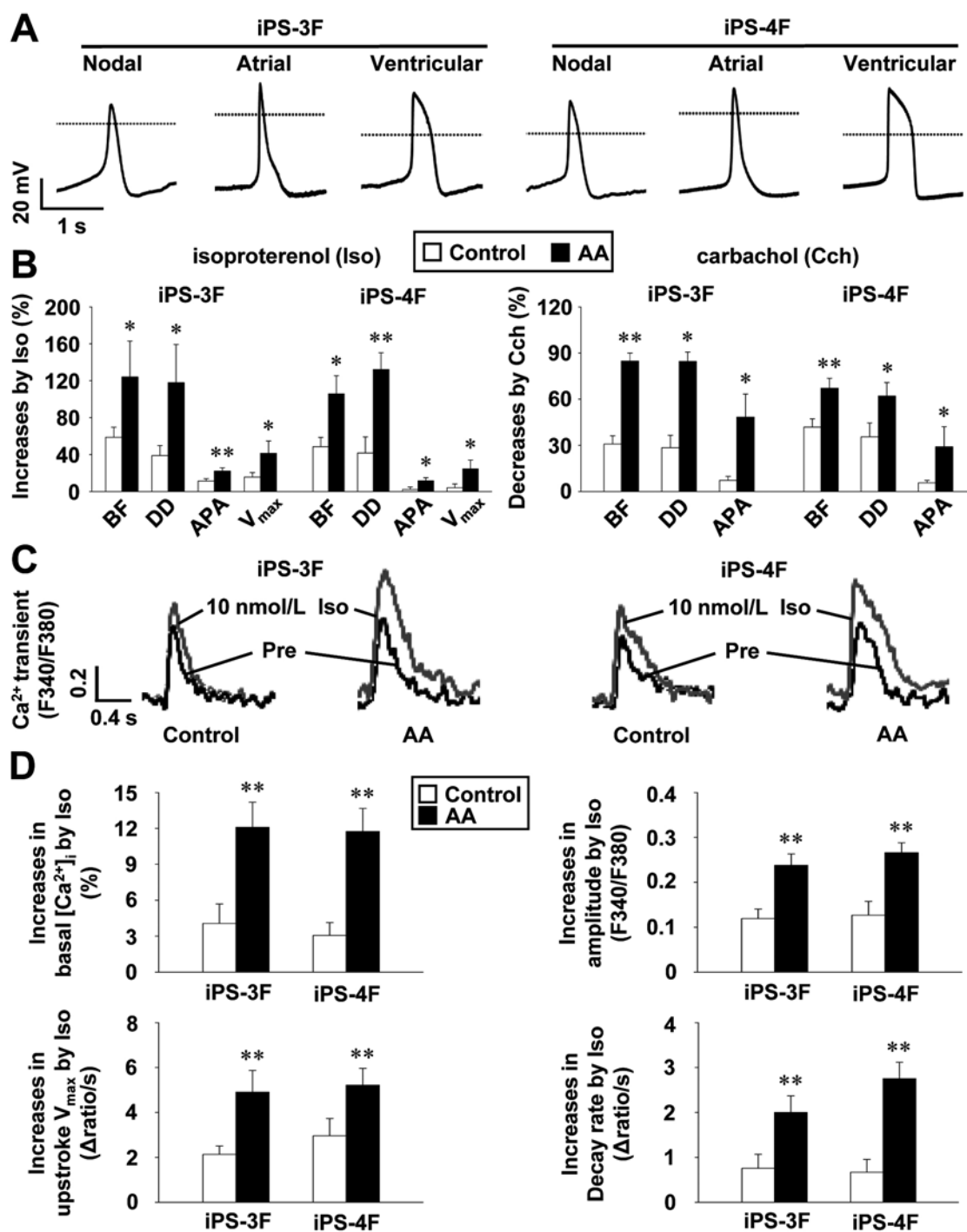
Figure 5 AA enhances the response of day 16-18 iPS-CMs to β-adrenergic and muscarinic stimulations. **(A)** Representative APs of AA-induced iPS-CMs showing characteristics of nodal-like, atrial-like, and ventricular-like APs. Dotted lines indicate 0 mV. **(B)** Comparison of Iso (10 nmol/l)-stimulated increases (left panel) and Cch (1 μmol/l)-induced decreases (right panel) in characteristics of APs between control and AA-applied iPS-CMs (*n* = 10-13). BF, beating frequency; DD, diastolic depolarization; APA, AP amplitude; V_{max}, maximum rise rate. **(C)** Representative tracings of spontaneous rhythmic Ca^{2+} transients with (grey) and without (black) Iso-simulation (10 nmol/l). **(D)** Iso-induced increases in basal $[Ca^{2+}]_i$, APA, upstroke V_{max}, and decay rate of Ca^{2+} transients in control or AA-applied iPS-CMs (*n* = 12-13). Data are expressed as means ± SEM. *$P < 0.05$, **$P < 0.01$ vs control.
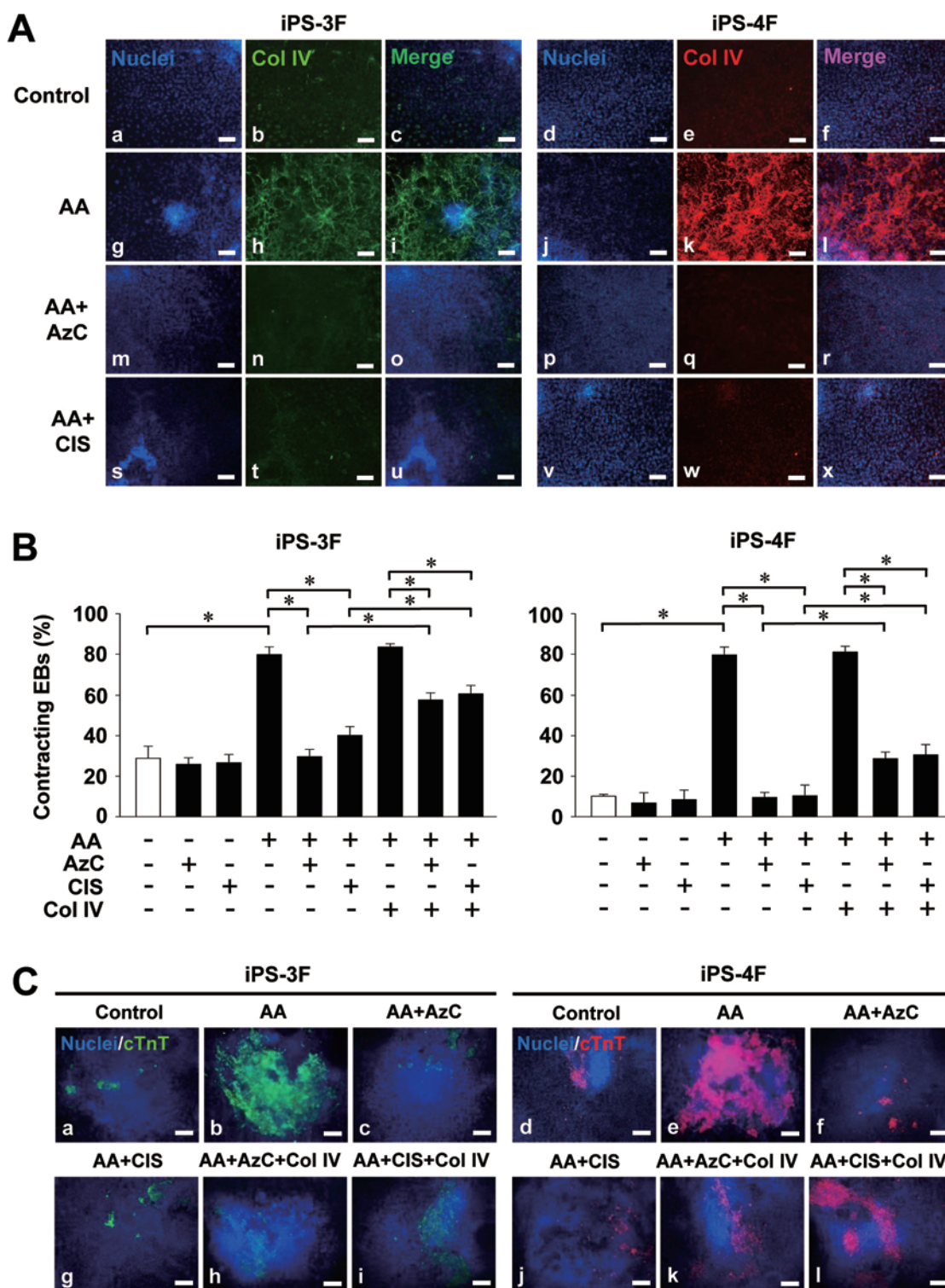
Figure 6 AA-enhanced collagen synthesis is required for its cardiomyocyte-promoting effect. **(A)** Immunostaining of Col IV at day-6 EBs treated with or without AA and collagen synthesis inhibitor AzC and CIS. **(B** and **C)** Cardiomyocyte-promoting effect of AA was abolished by AzC and CIS, and could be partially rescued by Col IV. Scale bars = 100 μm. Nuclei were counterstained with Hoechst33258 (blue). Data are expressed as means ± SEM. *$P < 0.01$ vs corresponding values.

two general collagen synthesis inhibitors, L-2-Azetidine carboxylic acid (AzC) and cis-4-hydroxy-D-proline (CIS) and found that the increased expression of Col IV and enhanced cardiomyocyte development by AA were completely abolished by AzC (50 μmol/l) and CIS (100 μmol/l) in both iPSC lines, while the blocking effects of AzC and CIS were partially rescued by directly plating the day-2 EBs onto Col IV-coated dishes (Figure 6A and 6B). These effects on cardiomyocyte formation were further confirmed by immunostaining of cTnT (Figure 6C). These data demonstrate that the collagen synthesis rather than antioxidative property of AA accounts for its promotive role in cardiac differentiation of iPSCs.

AA augments the cardiomyocyte population derived from iPSCs by specifically promoting the proliferation of CPCs in a collagen synthesis-dependent mechanism

Next, we attempted to elucidate further why AA-increased collagen expression promotes cardiac differentiation of iPSCs. Collagens are indispensible components of the extracellular matrix (ECM), which plays a critical role in cardiac development and function, and have been shown to affect cell proliferation and differentiation [8]. However, the effect of collagens on the proliferation and specification of CPCs is unclear. We found that day-10 iPS-CMs with double-immunostaining of BrdU and cTnT showed comparable percentages of double-positive cells between control and AA-applied groups (Figure 7A). Taken together with the observation that AA shows no cardiac-inducing effect when applied after differentiation day 6 (Figure 1B), these results suggest that AA treatment appears not to affect the proliferation of cardiomyocytes. As the most critical stage for AA to take effect is day 2-6 (Figure 1B), a crucial time for CPC specification, we then investigated the proliferation of day-5 CPCs by FACS analysis of Nkx2-5/BrdU double-staining cells. AA-treated EBs showed a markedly increased percentages of both Nkx2-5$^+$ and proliferating BrdU$^+$/Nkx2-5$^+$ CPCs, while the promoting effects were fully abrogated by AzC and CIS treatment (Figure 7B). Interestingly, the ratio of BrdU+/Nkx2-5$^-$ cells was not significantly altered by AA application (Figure 7B, right lower panel), indicating that this pro-proliferation effect of AA is restricted in CPCs. As ECM may affect cell survival [8], we also examined the apoptosis status of day-5 EBs and found that AA did not affect the apoptotic index and cell viability (Supplementary information, Figure S8).

To further assess whether this effect is directly mediated by AA or indirectly mediated by other cells, we isolated Flk1$^+$/Cxcr4$^+$ CPCs [34] by FACS from day-5 EBs and expanded them in the presence or absence of AA for 3 days. Schematic diagram of the strategy for analyzing the role of AA in expansion or differentiation of the CPCs was shown in Supplementary information, Figure S9A. We found that AA markedly increased the number of Mef2c$^+$ CPCs and the level of BrdU incorporation in these cells (Figure 7C), whereas it did not affect the cardiac differentiation capacity of sorted CPCs (Supplementary information, Figure S9B). These data further prove that AA enhances cardiogenesis of iPSCs mainly through promoting the proliferation of CPCs.

AA enhances CPC proliferation via the MEK-ERK1/2 pathway

We next sought to identify signaling pathways involved in AA-mediated CPC proliferation by using specific signaling inhibitors. The AA-enhanced BrdU$^+$/Nkx2-5$^+$ CPC population remained unchanged when addition of JNK, JAK, PI3K, or p38MAPK inhibitor, whereas the MEK inhibitor completely abolished AA-induced increases of BrdU$^+$/Nkx2-5$^+$ CPCs and contracting EBs (Figure 7D), suggesting that the MEK-ERK1/2 pathway is involved in the AA-dependent CPC expansion and cardiomyocyte augmentation. This was confirmed by the strongly increased phosphorylation of ERK1/2 in AA-treated cells at differentiation day 5 and this effect was eliminated by the collagen synthesis inhibitors AzC and CIS (Supplementary information, Figure S10). Noticeably, p38MAPK inhibitor suppressed AA-enhanced cardiomyocyte differentiation, but not the proliferation of CPCs (Figure 7D), which is consistent with the observation in mESCs [35], and suggesting that the involvement of p38MAPK pathway in cardiac differentiation is independent of the proliferation of CPCs.

Taken together, these data reveal that AA-induced collagens synthesis enhances the differentiation of iPSCs into cardiomyocytes through specifically promoting the CPC proliferation via MEK-ERK1/2 pathway.

AA remarkably enhances the cardiac differentiation of hiPSCs

To further investigate whether the cardiomyocyte-promoting effect of AA is conserved in human, we examined its role on hiPSC line hAFDC-iPS-36 [36]. Figure 8A showed typical morphology of undifferentiated hiPSC clones. AA treatment at 50 μg/ml during day 0-30 robustly enhanced both the percentage of contracting EBs and cTnT$^+$ cardiomyocytes in hiPSCs (Figure 8B and 8C). This effect was further confirmed by the enhanced expression of cardiac genes *NKX2-5*, *TBX5*, *TNNT2*, *MYL3*, *SLC8A1*, *CACNA1A* (Figure 8D), and myofilamental
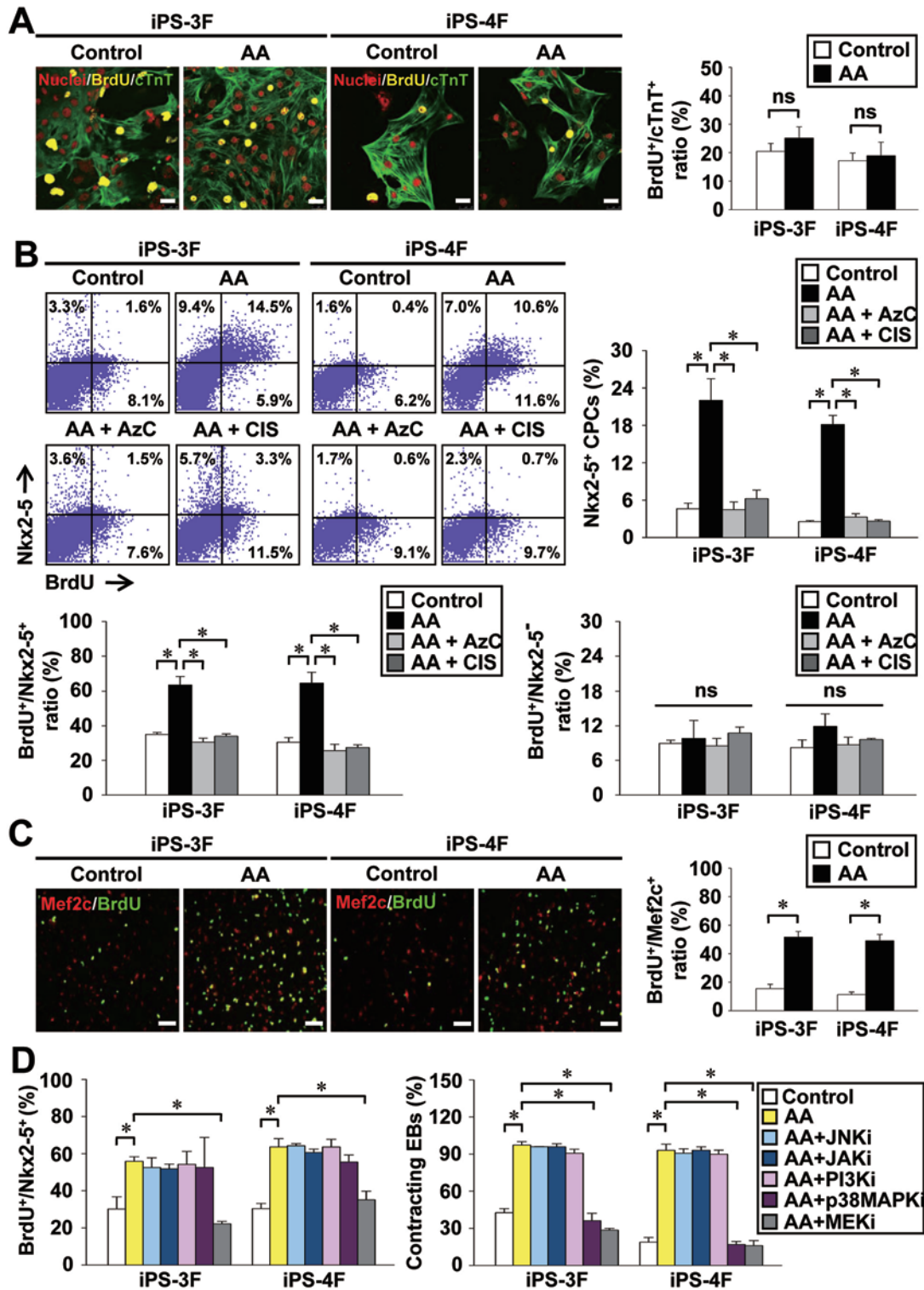
Figure 7 AA specifically enhances the proliferation of CPCs in a collagen synthesis-dependent manner. **(A)** Immunostaining of cTnT and BrdU in day-10 iPS-CMs. Data were quantified from 6-8 random fields in two assays. Scale bars = 25 μm. Nuclei were counterstained with PI (red). **(B)** Double staining of Nkx2-5 and BrdU at day-5 ($n = 3$). **(C)** Immunostaining of Mef2c and BrdU in day-8 CPCs (3 days after sorting). Data were quantified from five random fields in two assays. Scale bars = 100 μm. **(D)** Effects of signal inhibitors on proliferation of Nkx2-5$^+$ CPCs and percentage of contracting EBs ($n = 3$). Data are expressed as means ± SEM. *$P < 0.01$ vs corresponding values. ns, no significant difference.
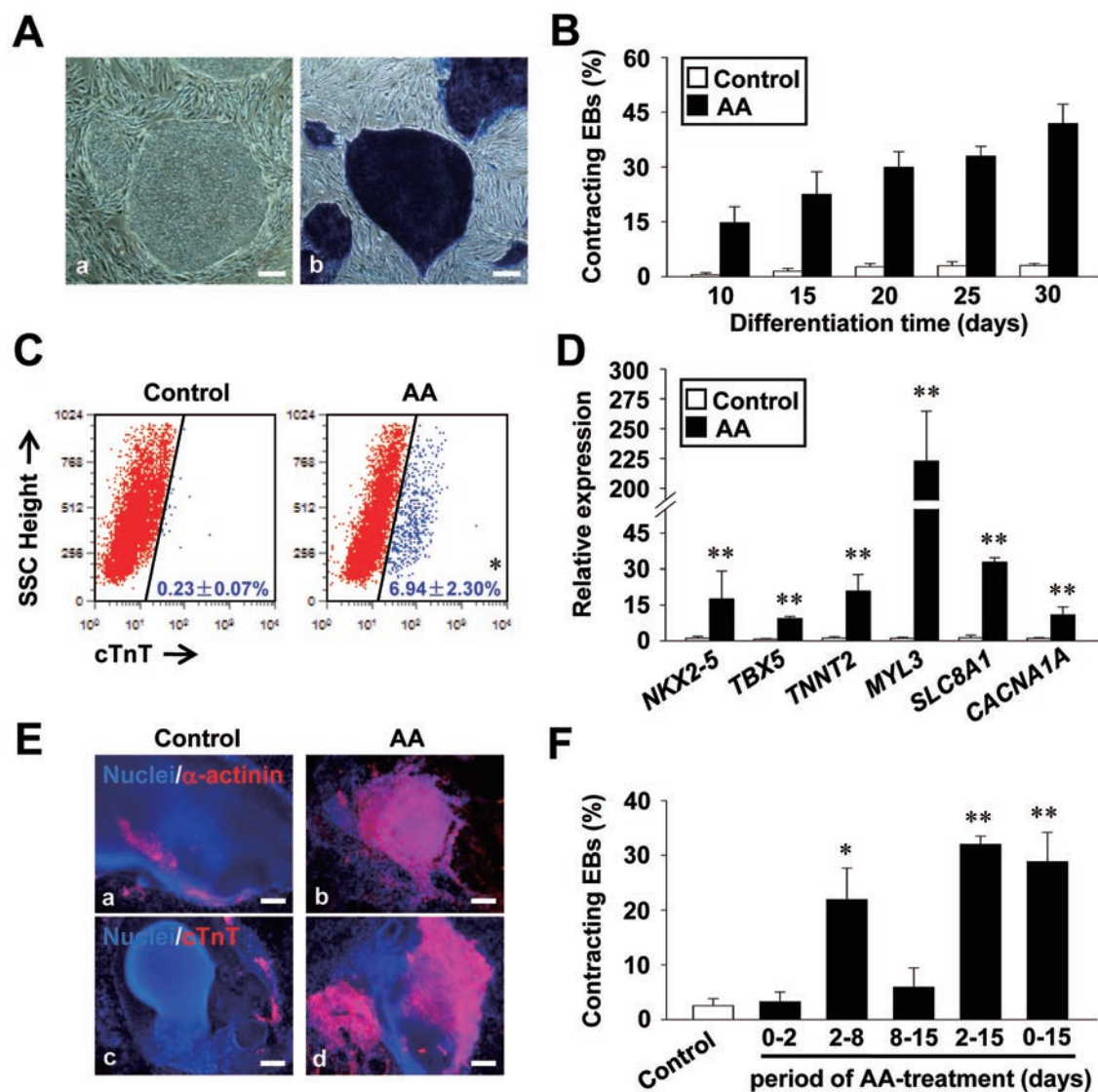
Figure 8 AA promotes cardiogenesis of human iPSCs (hiPSCs). **(A)** Morphology (a) and alkaline phosphatase staining (b) of undifferentiated hiPSCs colonies. **(B)** Percentages of contracting EBs during differentiation. **(C)** Percentages of cTnT⁺ cardiomyocytes in hiPSC-derived EBs at day 30. **(D, E)** Quantitative RT-PCR **(D)** and immunostaining **(E)** analysis showed the remarkable increases in expression of cardiac markers following AA treatment (*n* = 3). **(F)** Time windows for AA-promoted cardiogenesis. Scale bars = 100 μm. Nuclei were counterstained with Hoechst33258 (blue). *$P < 0.05$, **$P < 0.01$ vs control.

protein markers α-actinin and cTnT (Figure 8E). Optimal treatment-phase analysis also proved the CPC specification period (day 2-8) to be the most critical time-window for AA to take effect (Figure 8F). These data indicate that AA promotes cardiac differentiation in both miPSCs and hiPSCs through stimulating the proliferation of CPCs.

Discussion

Our findings here extend previous knowledge of AA in promoting the cardiac differentiation of ESCs [25-27],

indicating that AA is an ideal cardiomyocyte inducer of both miPSCs and hiPSCs, and reveal a novel cardiomyocyte-promoting mechanism. The important findings are that (i) only AA shows consistent cardiac-inducing capacity among different iPSC lines including those without spontaneous cardiogenic potential and remarkably enhances the cardiac differentiation of both miPSCs and hiPSCs; (ii) the cardiomyocyte-promoting effect is also seen in large-scale generated and serum-free cultivated EBs; (iii) such effect of AA is restricted to the phase of CPC specification and is attributed to the collagen

synthesis-based increase of CPC proliferation via MEK-ERK1/2 pathway; (iv) AA facilitates the *in vitro* expansion of CPCs isolated from iPSCs; and (v) AA improves structural and functional maturation of iPS-CMs. Therefore, by using AA, a straightforward, economical, and efficient system has been successfully established from which significant amount of CPCs and functional cardiomyocytes could be produced from various iPSC lines.

Cardiomyocytes can be successfully obtained from iPSCs, however the differentiation efficiency is low and a huge interline variability is observed [11, 12, 16, 17]. Moreover, the diverse levels of endogenous signaling between different iPSC lines make them difficult to be universally manipulated by exogenous cytokines [14]. AA has been well documented to promote cardiac differentiation of ESCs [25-27]. Here, we demonstrate, for the first time, the conclusive and universal role of AA in cardiac differentiation of iPSCs and provide novel insight into the underlying mechanism. Most of the existing cardiac differentiation protocols, especially for human ESCs, require a complicated switch of culture condition, addition of expensive cytokines and signal inhibitors at accurate timing and concentration, or co-culture with stroma cells [7]. To develop an easily practicable and universal system suitable for the efficient cardiac differentiation of iPSCs, we performed single factor-based screening to make the system as simple as possible. It is noteworthy that only AA shows the uniform and robust cardiomyocyte-promoting effect among all of the iPSC lines tested, including the lines that failed to differentiate into cardiomyocytes spontaneously in our screening. With the simple supplement of AA, a relative large amount of cardiomyocytes is efficiently generated from ESCs [25-27] and iPSCs, suggesting that AA is a suitable cardiomyocyte inducer of pluripotent stem cells for both scientific and economical reasons.

The most successful cardiac differentiation approaches to date are those focusing on the induction of CPCs [28, 37]. Our observations of AA is not only increasing the percentage of iPSC-derived CPCs but also specifically promotes their proliferation by manipulating the microenvironment (Figure 7), further proving the importance of manipulating CPCs in guiding efficient cardiac differentiation. ECM and MEK-ERK1/2 pathway have been shown to be involved in the proliferation of cardiomyocytes [38]. Our data here, for the first time, link the ECM to the control of CPC fate and show that the MEK-ERK1/2 pathway is activated by AA by regulating collagen synthesis and plays an important role in stimulating proliferation of the CPCs derived from iPSCs. Moreover, the possibility to generate patient-specific CPCs from iPSCs offers exciting novel

routes in the field of cardiac translational medicine and drug discovery. iPSC-derived multipotent CPCs, which possess better proliferation capacity and can differentiate into multiple lineages of the heart, might offer an advantage over mere cardiomyocytes, as they contribute to both muscularization and vascularization [20]. However, one of the major limitations for their utilization is the difficulty in CPC expansion. Here, we provide a simple and effective method for the *in vitro* expansion of CPCs isolated from iPSCs by utilizing AA. This approach may facilitate the cloning of CPCs or direct transdifferentiation of somatic tissues into CPCs. Whether AA would affect the proliferation of other types of cardiovascular progenitors needs to be further examined.

We showed here that alternative antioxidants (including Vb1, GMEE and NAC) failed to mimic the cardiomyocyte-promoting role of AA in iPSCs (Supplementary information, Figure S6A). This is consistent with previous observations showing the inability of alternative antioxidative agents, such as 4,5-dihydroxy-1,3-benzene-disulfonic acid, vitamin E [26] or NAC [25], to mimic the effect of AA on the cardiac differentiation of ESCs. These observations suggest that the cardiac promoting role of AA is independent of its antioxidative property, or at least, that its antioxidative effect is insufficient to induce cardiac differentiation of the ESCs and iPSCs. Paradoxically, Crespo *et al.* [39] observed that antioxidants including NAC and mitoubiquinone hampered the cardiac differentiation of ESCs. Those inconsistent findings may be caused by the different cell lines and differentiation conditions, such as different batch of serum used in each study. In addition, they found that the impaired cardiac differentiation induced by antioxidants or low glucose (5 mM) culture condition, which resulted in a decrease of reactive oxygen species (ROS) production, could be rescued by AA. Thus, they attributed the cardiomyocyte-promoting effect of AA to its ability in increasing ROS level [39]. However, this could be alternatively explained that this rescue effect of AA may be mediated by the increased synthesis of collagen, which has been proved critical to the cardiomyocyte-promoting role of AA in previous [25] studies as well as ours. This hypothesis is further confirmed by the fact that AA 2-phosphate (A2-P), a stable form of AA but without pro-oxidant effect [40], also robustly enhances the cardiac differentiation of ESCs [25]. Moreover, we demonstrated here that the increased cardiac differentiation and proliferation of the CPCs, as well as the robust activation of MEK-ERK1/2 pathway, could be eliminated by the collagen synthesis inhibitors AzC and CIS (Figures 6, 7 and Supplementary information, Figure S10). Taken together, those data sup-

port that the collagen synthesis rather than the antioxidative property of AA accounts for its cardiac promoting role in iPSCs.

Maturation of pluripotent stem cell-derived cardiomyocytes is critical for their application in either drug screen or cell transplantation. However, iPS-CMs are not only immature compared with the ESCs- or fetal heart-derived ones, but also more resistant to maturation methods that work effectively for ESC-derived cardiomyocytes [6, 18, 19]. Interestingly, AA promotes the maturation of iPS-CMs characterized by the rapid decrease of contracting EBs after differentiation day 17 (Figure 1C). This is further supported by the fact that AA-induced iPS-CMs show better sarcomeric organization (Figure 2B) and higher responses to β-adrenergic and muscarinic stimulations (Figure 5). The underlying mechanism may be related to its role in promoting accumulation of ECM proteins that have been shown to improve the maturation of ESC-derived cardiomyocytes [41]. Alternatively, this effect may be related to the accelerated dynamics of cardiac differentiation or activation of particular transcriptional program and signaling pathways following AA treatment. These possibilities need to be further investigated. Taken together, our findings reveal the role of AA in promoting the maturation of iPSC-CMs and provide the first pro-maturation method that works in iPS-CMs to our knowledge.

Besides the *in vitro* application, AA has been reported to improve cardiomyoblast propagation and promote vascularization in bioartificial grafts *in vivo* [42], which can be explained by our findings that AA activates CPCs that are capable of differentiating into multiple cardiovascular cells. Thus, it is fascinating to elucidate whether AA could facilitate transplantation of iPSC-derived CPCs and has the potential to activate endogenous CPCs *in vivo* in the future.

In summary, our findings demonstrate that AA is a suitable cardiomyocyte inducer of iPSCs *in vitro* and robustly enhances the cardiac differentiation of both miPSCs and hiPSCs. Moreover, AA minimizes the interline variance in cardiogenic capacity of iPSCs and facilitates the structural and functional maturation of iPS-CMs. In addition, we have proved that AA specifically promotes the proliferation of iPSC-derived CPCs via MEK-ERK1/2 pathway by increasing the collagen synthesis, which also offers a novel method for the *in vitro* expansion of CPCs. The discoveries in this study are useful to fully harness the unrivaled potential of iPSCs in scientific studies, drug discovery, and toxicity testing, and patient-specific cardiac regenerative medicine.

Materials and Methods

Culture and differentiation of mouse iPSCs (miPSCs)

All miPSC lines used in this study were routinely maintained in standard ESC medium containing 15% FBS (Hyclone, Logan, UT, USA), 1 µmol/l non-essential amino acids, 1 mmol/l Glutamine, 100 µmol/l β-mercaptoethanol, 50 U/ml penicillin, and 50 mg/ml streptomycin on mitomycin-C-treated mouse embryonic fibroblast (MEF) feeder layers in the presence of leukemia inhibitory factor (Millipore, Billerica, MA, USA, 1 000 U/ml). Differentiation of the iPSCs was initiated by the classical hanging-drop method as described previously [29]. The formed EBs were harvested 2 days later and then transferred into ultralow attachment plates (Corning, Canton, NY, USA) for 3 days of suspension culture. Then the EBs were seeded onto gelatin-coated plates for adhered culture and examinations. For large-scale generation of EBs, iPSCs were trypsinized and seeded onto non-attach petri dishes at a density of 10^5 cells/ml and the auto-aggregated EBs were plated onto gelatin-coated plates at day 5. For differentiation of the iPSCs in serum-free conditions, EBs were induced to form in medium containing 2.5% Knockout Serum Replacement (KSR, Invitrogen, Carlsbad, CA, USA) by hanging-drop method. BMP4 (R&D Systems, Minneapolis, MN, USA) was added from day 2-5 at 10 ng/ml to induce cardiomyocytes formation. All cytokines used were purchased from R&D Systems. AA (Sigma, St. Louis, MO, USA) was added during the entire differentiation period at 50 µg/ml unless otherwise indicated. Medium was renewed every 2-3 days. All cultivation medium/substances for cell cultures were from Invitrogen BRL if not indicated.

Culture and differentiation of hiPSCs

Undifferentiated hiPSCs [36] were maintained on inactivated MEFs at a density of 2×10^4 cells/cm² in DMEM/F12 containing 20% KSR and 4 ng/ml bFGF (Sigma) as described previously [12]. The hiPSCs were passaged onto a low-density MEF feeder layers (1.3×10^4 cells/cm²) and expanded for 3-4 days before differentiation. Colonies were then detached from the feeder layer by dispase (Invitrogen) and seeded onto ultralow attachment plates in hESCs culture medium without bFGF to induce EB formation. At day 2, the medium was replaced with differentiation medium containing 20% FBS (EB20) and the EBs were plated onto gelatin-coated plates at day 5. The FBS concentration was reduced to 5% (EB5) at day-10 and the medium was changed every 4-5 days. AA was added during the entire differentiation period at 50 µg/ml.

Reverse transcription (RT)-PCR and quantitative qRT-PCR

Total RNA was extracted from different samples using an RNeasy Plus Mini Kit (QIAGEN, Valencia, CA, USA) following the manufacturer's instructions and treated with DNAse I (Promega, Madison, WI, USA) for 15 min to eliminate the potential contamination of genomic DNA. cDNA was generated by reverse-transcribed total RNA (1 µg) using oligo (dT) primer and Rever-Tra Ace reverse transcriptase (Toyobo, Osaka, Japan). PCR was carried out using Taq DNA Polymerase (Takara, Shiga, Japan). The PCR primers are listed in Supplementary information, Table S3. *m28s* was used as endogenous control, and samples without reverse transcription were used as negative controls. Q-PCR was performed and analyzed by kinetic real-time PCR using the ABI PRISM 7900 system (Applied Biosystems, Foster City, CA, USA)

with SYBR Green Realtime PCR Master Mix plus (Toyobo) for relative quantification of the indicated genes. The transcript of *Gapdh* was used for internal normalization. The qRT-PCR primers are listed in Supplementary information, Table S4.

Flow-cytometry analysis and cell sorting

Undifferentiated iPSCs or EBs were harvested and dissociated by Non-enzyme Cell Dissociation Buffer (Invitrogen). Samples were then stained for the presence of appropriate membrane markers including: SSEA1 (1:200; Millipore), PE-conjugated CD31 (1:200; eBioscience, San Diego, CA, USA), PE-conjugated CD41 (1:200; eBioscience) or isotype-matched negative control. Alexa Fluor 594 goat anti-mouse IgMs (1:1 000, Invitrogen) were used as secondary antibody to visualize SSEA1. To detect the intracellular antigen, cells were fixed and permeabilized by Foxp3 Staining Buffer Set (eBioscience), blocked by 5% FBS and incubated with primary antibody of cTnT (1:100; Abcam, La Jolla, CA, USA) and α-SMA (1:100, Sigma). Isotype-matched IgGs (BD Biosciences, Bedford, MA, USA) were used as negative control. DyLight 549-conjugated antibodies (Jackson ImmunoResearch, West Grove, PA, USA) were used as secondary antibody. Cells were then analyzed and quantified by flow cytometry (FACStar Plus Flow Cytometer, BD Biosciences).

For cell sorting, live cells were harvested and double-stained with APC-conjugated Flk1 (1:200, BD Biosciences) and PE-conjugated Cxcr4 (1:50, BD Biosciences). Flk1$^+$/Cxcr4$^+$ cells were then sorted by flow cytometry and plated onto gelatin-coated plates for proliferation determination. For differentiation assays, cells were seeded onto U-bottom ultralow attachment 96-well plates (Corning) at a density of 5 000 cells/well to induce the formation of reaggregates in OP9 stroma cells-conditioned medium containing 5% FBS, 100 ng/ml DKK1 (R&D Systems), and 10 ng/ml VEGF (R&D Systems). Cardiac differentiation efficiency was estimated by flow cytometry at differentiation day 15 (10 days after sorting). For cardiomyocytes purification, cells were dispersed and stained by 10 nmol/l TMRM (Invitrogen) with stirring for 30 min, then analyzed and sorted by flow cytometry [33].

Immunocytochemical staining analysis

ALP activity was analyzed by staining with an ALP substrate kit III (Vector Laboratories, Burlingame, CA, USA) according to the manufacturer's instructions. Immunostaining assays were performed according to the protocol described before [43]. Briefly, cells were fixed with 4% paraformaldehyde, permeabilized in 0.3% Triton X-100 (Sigma), blocked in 10% normal goat serum (Vector Laboratories) and then incubated with primary antibodies against Oct4 (1:200), SSEA1 (1:200; Millipore), α-actinin (1:300; Sigma), cTnT (1:300; Abcam), and Col IV (1:200; Abcam) in 4 °C overnight and detected by Alexa Fluor 594 goat anti-mouse IgMs, and DyLight 488- or DyLight 549-conjugated secondary antibodies. Nuclei were stained with Hoechst33258 (Sigma) and staining with normal goat serum was used to be a negative control. A Nikon TS100 fluorescence microscope or Leica TCS SP2 confocal laser-scanning microscope was used for slide observing and image capture.

Plasmid construction and cell transfection

siRNAs constructs in the pLKO.1-Puro plasmid system for lentivirus-mediated gene knockdown were obtained from Sigma.

siRNA sequence were obtained from TRC Library Database (Sigma) and listed in Supplementary information, Table S5. Viral production and infection were performed according to standard protocol. Puromycin selection was applied continuously during all subsequent cell culture including differentiation.

Proliferation and apoptosis assays

Proliferation status of the cells was determined by measuring the incorporation of BrdU. Cells were incubated with 100 μmol/l BrdU (Sigma) and BrdU labeling was detected by confocal laser scanning microscope or flow cytometry using an FITC or APC-conjugated anti-BrdU antibody (BD Biosciences), following the immunostaining protocols. Staining of samples without BrdU addition was used as negative control. Double staining of BrdU with Nkx2-5 and Mef2c was performed by Nkx2-5 (1:100; Santa Cruz Biotechnology, Santa Cruz, CA, USA) and Mef2c (1:100; Cell Signaling, Beverly, MA, USA) antibody. Signal inhibitors used in this assay were 10 μmol/l JNK inhibitor SP600125 (Calbiochem, Gibbstown, NJ, USA), 50 μmol/l JAK inhibitors AG490 (Sigma), 20 μmol/l PI3K inhibitor Wortmannin (Calbiochem), 10 μmol/l p38MAPK inhibitor SB203580 (Calbiochem), and 1 μmol/l MEK inhibitor PD0325901 (Stemgent, San Diego, CA, USA) according to previous publication [44].

To determine the apoptosis status of the cells, TUNEL staining was performed with the in situ Cell Death Detection kit (Roche, Mannheim, Germany) according to the manufacturer's instruction. Annexin V-PI double-stainings performed with PI (0.5 μg/ml) and APC-labeled Annexin V antibody (1:20; BD Biosciences) were further used to evaluate the apoptosis and necrosis levels. Cells were analyzed and quantified by flow cytometry.

Whole cell patch clamp

Whole cell patch clamps using EPC-10 amplifier (Heka Electronics, Bellmore, NY, USA) in current clamp mode were used to record APs in spontaneously beating iPS-CMs following the method described previously [43]. For AP recording, the pipette electrode (2~6 MΩ) were filled with a solution containing (mmol/l): 50 KCl, 80 K-Asparate, 5 MgCl$_2$, 5 EGTA, 10 Hepes, 5 Na$_2$ATP (pH 7.2 adjusted with KOH); the extracellular bathing solution containing (mmol/l): 135 NaCl, 5.4 KCl, 1.8 CaCl$_2$, 1.0 MgCl$_2$, 10.0 glucose and 10.0 HEPES (pH 7.4, adjusted with NaOH). The glass coverslips containing the cells were placed onto a temperature-controlled (35 °C) recording chamber and perfused continuously with extracellular solution.

Measurement of Ca^{2+} transients

Isolated mouse iPS-CMs were loaded with 5 μmol/l fura-2 AM and 0.45% pluronic F-127 (Molecular Probes, Eugene, OR, USA) for 10 min and washed in extracellular solution for 15 min at 35 °C room temperature. The cells were perfused continuously with extracellular solution at 35 °C. Fluorescence signals of fura-2 were detected by a Fluorescence System (IonOptix, Milton, MA). After subtraction of background fluorescence, the 340- to 380-nm fluorescence ratio (R) was recorded and analyzed by IonWizard 6.0 software (IonOptix).

Immunoblot analysis

Immunoblot analyses were performed according to the protocol described previously [45]. Protein samples were size fractionated

by SDS-polyacrylamide gel electrophoresis and the separated proteins were electrophoretically transferred to polyvinylindene difluoride membranes (Bio-Rad, Hercules, CA, USA). Then the membrane was incubated with primary antibodies against p-ERK1/2 (1:1 000; Santa Cruz Biotechnology), total ERK1/2 (1:1 000; Cell Signaling), RyR2 (1:1 000; Abcam), SERCA2 (1:1 000; Santa Cruz Biotechnology), Phospholamban (1:2 000; Millipore), Connexin43 (1:500; Invitrogen), and GAPDH (1:1 000; Santa Cruz Biotechnology). Horseradish peroxidase-linked anti-rabbit (1:4 000; Santa Cruz Biotechnology) or anti-mouse antibodies (1:4 000; Sigma) were used as secondary antibodies.

Statistical analysis

Data were presented as means ± SEM. Statistical significance of differences was estimated by one way ANOVA or Student's *t* test by SigmaStat 3.5 software (Sigma). $P < 0.05$ was considered significant.

Acknowledgments

References

1   Yu J, Vodyanik MA, Smuga-Otto K, *et al.* Induced pluripotent stem cell lines derived from human somatic cells. *Science* 2007; **318**:1917-1920.

2   Takahashi K, Tanabe K, Ohnuki M, *et al.* Induction of pluripotent stem cells from adult human fibroblasts by defined factors. *Cell* 2007; **131**:861-872.

3   Takahashi K, Yamanaka S. Induction of pluripotent stem cells from mouse embryonic and adult fibroblast cultures by defined factors. *Cell* 2006; **126**:663-676.

4   Nelson TJ, Martinez-Fernandez A, Yamada S, *et al.* Repair of acute myocardial infarction by human stemness factors induced pluripotent stem cells. *Circulation* 2009; **120**:408-416.

5   Nsair A, Maclellan WR. Induced pluripotent stem cells for regenerative cardiovascular therapies and biomedical discovery. *Adv Drug Deliv Rev* 2011; **63**:324-330.

6   Kong CW, Akar FG, Li RA. Translational potential of human embryonic and induced pluripotent stem cells for myocardial repair: insights from experimental models. *Thromb Haemost* 2010; **104**:30-38.

7   Vidarsson H, Hyllner J, Sartipy P. Differentiation of human embryonic stem cells to cardiomyocytes for *in vitro* and *in vivo* applications. *Stem Cell Rev* 2010; **6**:108-120.

8   Bowers SL, Banerjee I, Baudino TA. The extracellular matrix: at the center of it all. *J Mol Cell Cardiol* 2010; **48**:474-482.

9   Mauritz C, Schwanke K, Reppel M, *et al.* Generation of functional murine cardiac myocytes from induced pluripotent stem

cells. *Circulation* 2008; **118**:507-517.

10 Narazaki G, Uosaki H, Teranishi M, *et al.* Directed and systematic differentiation of cardiovascular cells from mouse induced pluripotent stem cells. *Circulation* 2008; **118**:498-506.

11 Zwi L, Caspi O, Arbel G, *et al.* Cardiomyocyte differentiation of human induced pluripotent stem cells. *Circulation* 2009; **120**:1513-1523.

12 Zhang J, Wilson GF, Soerens AG, *et al.* Functional cardiomyocytes derived from human induced pluripotent stem cells. *Circ Res* 2009; **104**:e30-e41.

13 Fujiwara M, Yan P, Otsuji TG, *et al.* Induction and enhancement of cardiac cell differentiation from mouse and human induced pluripotent stem cells with cyclosporin-a. *PLoS One* 2011; **6**:e16734.

14 Kattman SJ, Witty AD, Gagliardi M, *et al.* Stage-specific optimization of activin/nodal and BMP signaling promotes cardiac differentiation of mouse and human pluripotent stem cell lines. *Cell Stem Cell* 2011; **8**:228-240.

15 Burridge PW, Thompson S, Millrod MA, *et al.* A universal system for highly efficient cardiac differentiation of human induced pluripotent stem cells that eliminates interline variability. *PLoS One* 2011; **6**:e18293.

16 Kaichi S, Hasegawa K, Takaya T, *et al.* Cell line-dependent differentiation of induced pluripotent stem cells into cardiomyocytes in mice. *Cardiovasc Res* 2010; **88**:314-323.

17 Martinez-Fernandez A, Nelson TJ, Ikeda Y, Terzic A. c-MYC independent nuclear reprogramming favors cardiogenic potential of induced pluripotent stem cells. *J Cardiovasc Transl Res* 2010; **3**:13-23.

18 Xi J, Khalil M, Shishechian N, *et al.* Comparison of contractile behavior of native murine ventricular tissue and cardiomyocytes derived from embryonic or induced pluripotent stem cells. *FASEB J* 2010; **24**:2739-2751.

19 Kuzmenkin A, Liang H, Xu G, *et al.* Functional characterization of cardiomyocytes derived from murine induced pluripotent stem cells *in vitro*. *FASEB J* 2009; **23**:4168-4180.

20 Lam JT, Moretti A, Laugwitz KL. Multipotent progenitor cells in regenerative cardiovascular medicine. *Pediatr Cardiol* 2009; **30**:690-698.

21 van Laake LW, Qian L, Cheng P, *et al.* Reporter-based isolation of induced pluripotent stem cell- and embryonic stem cell-derived cardiac progenitors reveals limited gene expression variance. *Circ Res* 2010; **107**:340-347.

22 Moretti A, Bellin M, Jung CB, *et al.* Mouse and human induced pluripotent stem cells as a source for multipotent Isl1+ cardiovascular progenitors. *FASEB J* 2010; **24**:700-711.

23 Chin MH, Mason MJ, Xie W, *et al.* Induced pluripotent stem cells and embryonic stem cells are distinguished by gene expression signatures. *Cell Stem Cell* 2009; **5**:111-123.

24 Noseda M, Peterkin T, Simoes FC, Patient R, Schneider MD. Cardiopoietic factors: extracellular signals for cardiac lineage commitment. *Circ Res* 2011; **108**:129-152.

25 Sato H, Takahashi M, Ise H, *et al.* Collagen synthesis is required for ascorbic acid-enhanced differentiation of mouse embryonic stem cells into cardiomyocytes. *Biochem Biophys Res Commun* 2006; **342**:107-112.

26 Takahashi T, Lord B, Schulze PC, *et al.* Ascorbic acid enhances differentiation of embryonic stem cells into cardiac

myocytes. *Circulation* 2003; **107**:1912-1916.

27 Chan SS, Chen JH, Hwang SM, *et al.* Salvianolic acid B-vitamin C synergy in cardiac differentiation from embryonic stem cells. *Biochem Biophys Res Commun* 2009; **387**:723-728.

28 Yang L, Soonpaa MH, Adler ED, *et al.* Human cardiovascular progenitor cells develop from a KDR+ embryonic-stem-cell-derived population. *Nature* 2008; **453**:524-528.

29 Boheler KR, Czyz J, Tweedie D, *et al.* Differentiation of pluripotent embryonic stem cells into cardiomyocytes. *Circ Res* 2002; **91**:189-201.

30 Zhao XY, Li W, Lv Z, *et al.* iPS cells produce viable mice through tetraploid complementation. *Nature* 2009; **461**:86-90.

31 Qin D, Gan Y, Shao K, *et al.* Mouse meningiocytes express Sox2 and yield high efficiency of chimeras after nuclear reprogramming with exogenous factors. *J Biol Chem* 2008; **283**:33730-33735.

32 Huang J, Chen T, Liu X, *et al.* More synergetic cooperation of Yamanaka factors in induced pluripotent stem cells than in embryonic stem cells. *Cell Res* 2009; **19**:1127-1138.

33 Hattori F, Chen H, Yamashita H, *et al.* Nongenetic method for purifying stem cell-derived cardiomyocytes. *Nat Methods* 2010; **7**:61-66.

34 Nelson TJ, Faustino RS, Chiriac A, *et al.* CXCR4+/FLK-1+ biomarkers select a cardiopoietic lineage from embryonic stem cells. *Stem Cells* 2008; **26**:1464-1473.

35 Aouadi M, Bost F, Caron L, *et al.* p38 mitogen-activated protein kinase activity commits embryonic stem cells to either neurogenesis or cardiomyogenesis. *Stem Cells* 2006; **24**:1399-1406.

36 Li C, Zhou J, Shi G, *et al.* Pluripotency can be rapidly and efficiently induced in human amniotic fluid-derived cells. *Hum Mol Genet* 2009; **18**:4340-4349.

37 Bu L, Jiang X, Martin-Puig S, *et al.* Human ISL1 heart progenitors generate diverse multipotent cardiovascular cell lineages. *Nature* 2009; **460**:113-117.

38 Ieda M, Tsuchihashi T, Ivey KN, *et al.* Cardiac fibroblasts regulate myocardial proliferation through beta1 integrin signaling. *Dev Cell* 2009; **16**:233-244.

39 Crespo FL, Sobrado VR, Gomez L, Cervera AM, McCreath KJ. Mitochondrial reactive oxygen species mediate cardiomyocyte formation from embryonic stem cells in high glucose. *Stem Cells* 2010; **28**:1132-1142.

40 Duarte TL, Almeida GM, Jones GD. Investigation of the role of extracellular H2O2 and transition metal ions in the genotoxic action of ascorbic acid in cell culture models. *Toxicol Lett* 2007; **170**:57-65.

41 Baharvand H, Azarnia M, Parivar K, Ashtiani SK. The effect of extracellular matrix on embryonic stem cell-derived cardiomyocytes. *J Mol Cell Cardiol* 2005; **38**:495-503.

42 Martinez EC, Wang J, Gan SU, *et al.* Ascorbic acid improves embryonic cardiomyoblast cell survival and promotes vascularization in potential myocardial grafts *in vivo*. *Tissue Eng Part A* 2010; **16**:1349-1361.

43 Cao N, Liao J, Liu Z, *et al. In vitro* differentiation of rat embryonic stem cells into functional cardiomyocytes. *Cell Res* 2011; **21**:1316-1331.

44 Shimoji K, Yuasa S, Onizuka T, *et al.* G-CSF promotes the proliferation of developing cardiomyocytes *in vivo* and in derivation from ESCs and iPSCs. *Cell Stem Cell* 2010; **6**:227-237.

45 Liang J, Wang YJ, Tang Y, *et al.* Type 3 inositol 1,4,5-trisphosphate receptor negatively regulates apoptosis during mouse embryonic stem cell differentiation. *Cell Death Differ* 2010; **17**:1141-1154.

(**Supplementary information** is linked to the online version of the paper on the *Cell Research* website.)